Ellipsometric studies of the dielectric function of SnSe and a simple model of the electronic structure and the bonds of the orthorhombic IV-VI compounds

S. Logothetidis and H. M. Polatoglou
Solid State Section, Department of Physics, Aristotle University of Thessaloniki, GR-540 06 Thessaloniki, Greece
(Received 1 December 1986)

The dielectric function of the orthorhombic SnSe has been measured ellipsometrically in the 1.26–5.6-eV photon-energy region. The second derivatives, with respect to frequency, of the real and imaginary parts of the dielectric function are obtained numerically from the measured spectra for the electric vector **E** parallel to the **a** and **b** axes and used to determine the critical-point parameters. The critical-point parameters are found to show features similar to those of GeS. The effect of the air exposure on both the dielectric function and the ellipsometric angles, as well as the structure of the surface, have been studied by spectroscopic and "null" ellipsometry and electron microscopy, respectively. The results indicate the formation of an amorphous overlayer after cleavage. A simple model for the electronic structure of the IV-VI orthorhombic compounds is presented. The energy bands and the density of states of the model are calculated and compared with the known band structure and density of states. The bonding is found to be provided from p orbitals forming σ saturated bonds. The dielectric constant ϵ_0 is calculated for all the orthorhombic IV-VI compounds using this simple model. It is found that the theoretical estimates are close to the experimental values and follow the experimental trend.

I. INTRODUCTION

In recent years a number of optical spectroscopic techniques have been concerned with the optical properties and the electronic structure of the interesting layer-like orthorhombic IV-VI compounds (GeS, GeSe, SnS, and SnSe).[1–5]

Spectroscopic ellipsometry (SE) is recognized today as a good tool for the investigation of the bulk optical properties,[6,7] and surfaces[8] of isotropic materials. Recently SE has been extended and some anisotropic materials have also been studied.[9–13]

The IV-VI orthorhombic compounds are of interest, since they are intermediate between the three-dimensional and the two-dimensional materials. This has been deduced from an analysis of force constants from Raman and ir reflectivity measurements.[1] It is interesting to observe the degree of anisotropy of other properties, such as the dielectric functions. It is not clear whether GeS or SnSe would be more anisotropic from the reasons stated in the works of Ref. 1. This question will be addressed in the discussion of the present results. Since the dielectric tensor and the interband transitions of GeS,[12] along with their temperature dependence, have been recently measured using SE, it is of interest to make a similar study for SnSe. On the other hand, relatively little is known about the electronic structure and the nature of the bonding in the IV-VI orthorhombic compounds,[2,14–17] as compared to the cubic and rhombohedral IV-VI compounds.[18–19] Black phosphorous (black-P) is the homopolar analog of the IV-VI orthorhombic compounds and it is the most studied orthorhombic crystal. A review of the experimental and theoretical studies of black-P has been given by Morita,[20] with the recognition that research on black-P has just started. Recently some electronic properties of the cubic IV-VI compounds have been studied,[21] by using the linear combination of atomic orbitals (LCAO) method, with nearest-neighbor interactions. Analytical expressions for the electronic energies have been given and both the stability of the cubic structure and the optical spectra have been analyzed. Also using the above formalism, a structural map for the compounds with an average of five valence electrons per atom ($\langle 5e \rangle$) has been constructed,[22] along with a discussion of the differences in the bonding between the cubic and the orthorhombic $\langle 5e \rangle$ compounds. The orthorhombic $\langle 5e \rangle$ compounds have a complicated structure and no analytical study of their electronic properties is possible. It is therefore necessary to construct a simple model.

In the present work we report on the dielectric function of SnSe at room temperature for the two principal polarizations **E**$\|$**a** and **E**$\|$**b** axes, in the photon-energy range 1.26–5.6 eV (Sec. II). A standard line-shape analysis of the data is used to obtain the critical-point (CP's) parameters: the energies (E), broadenings (Γ), and strengths (A). Also experimental results are presented regarding the changes occurring at the surface of GeS and SnSe, due to the exposure of the crystals to the atmosphere. These changes are observed using SE and "null" ellipsometry measurements, and reflection high-energy electron diffraction (RHEED) (Secs. III and IV). A simple model for the electronic structure of the $\langle 5e \rangle$ compounds is proposed. Using this model we discuss the nature of the bonds and the electronic transitions which give the structure of the dielectric function (Sec. V). Also the static dielectric constant is calculated for all the $\langle 5e \rangle$ orthorhombic crystals.

II. EXPERIMENT

The SnSe crystals were grown by sublimation from polycrystalline material. The samples were prepared and measured as described in Refs. 12 and 13. Measurements were performed perpendicular to the c axis and each spectra was obtained from a fresh surface produced by peeling off some layers with adhesive tape. The SE measurements were performed with a rotating-analyzer ellipsometer. (Details about this particular system have been published elsewhere.[11]) During these measurements the samples were mounted in a windowless cell in flowing dry N_2. The total time after cleavage which was required to obtain a spectrum was about 15 min in the energy range 1.26–2.3 eV and about 30 min in the energy range 1.66–5.6 eV. The null ellipsometric measurements in air and at room temperature were performed with a Gaertner L-119X ellipsometer in the "PCSA configuration"[23] and the readings with this technique were taken in two zones.

III. DIELECTRIC FUNCTION AND CRITICAL-POINTS PARAMETERS

Ellipsometry measures the complex reflectance ratio, ρ, between the reflection coefficients r_p and r_s of light with its polarization parallel (p) and perpendicular (s) to the plane of incidence, at a given angle of incidence θ. This ratio is expressed as follows:

$$\rho = r_p / r_s = \tan\Psi \exp(i\Delta) . \quad (1)$$

The ratio ρ, in the case of a bulk cubic material, is directly related to the dielectric function $\epsilon(\omega)$ of the material through the expression

$$\epsilon(\omega) = \sin^2\theta \left[1 + \left[\frac{1-\rho}{1+\rho} \right]^2 \tan^2\theta \right] , \quad (2)$$

where a two-phase model is assumed.

In the case of an anisotropic material the dielectric function is a tensor. Its principal components can be obtained only from measurements on certain planes of incidence where the reflection matrix is diagonal.[23]

In cases where the crystal is anisotropic or there is an overlayer, the dielectric function as calculated by using Eq. (2) will be called the pseudodielectric function.

In a recent paper[12] we have described in detail the method to calculate all the principal components of the dielectric tensor in an orthorhombic material. To obtain only the two components of the dielectric tensor that correspond to polarizations parallel to the cleavage plane, namely (**a**,**b**) it is only necessary to use the approximate procedure suggested by Aspnes[9,24] and utilized in Refs. 12 and 13.

Figure 1 shows the real and imaginary parts of the pseudodielectric function in the two different orientations parallel to **a** and **b** axes for two angles of incidence that were measured in the energy region 1.66–5.6 eV. Each of the four spectra was received from a freshly cleaved surface, while a 20-meV photon-energy mesh was used for all cases. The results for the real and imaginary parts of the two principal components (ϵ_a,ϵ_b) of the dielectric tensor, as calculated by the procedure mentioned above, are shown in Figs. 2 and 3, respectively, together with the results of Ref. 25 in the energy range 1.26–5.6 eV. The spectra of the real and imaginary parts of the dielectric functions (ϵ_a,ϵ_b) shown in these figures are similar to the corresponding spectra of GeS.[12,13] They show the same number of peaks and shoulders and the presence of similarly broad peaks.

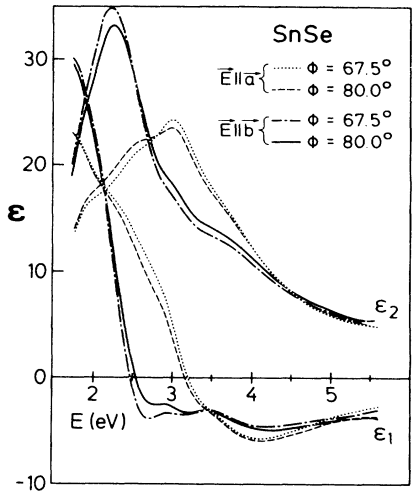

FIG. 1. Real (ϵ_1) and imaginary (ϵ_2) parts of the pseudodielectric function of SnSe from measurements with the ac and bc planes of incidence perpendicular to the cleavage plane at different angles of incidence.

There are large differences between our data and those of Ref. 25, as shown in Figs. 2 and 3. The spectra of the dielectric function of Ref. 25 in the above energy region have been calculated by Kramers-Kroning analysis of the optical-transmission spectra on thin cleaved platelets. It is well known that the sensitivity of the method used in Ref. 25 is not good at large energies, because it is

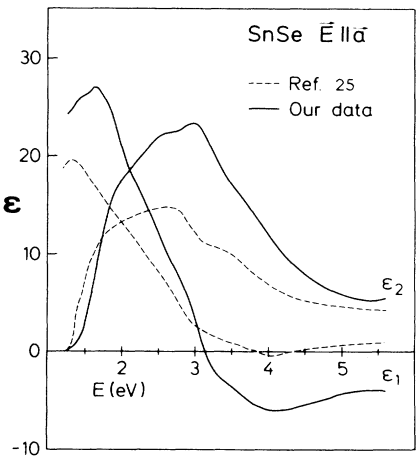

FIG. 2. Real and imaginary parts of the dielectric function of SnSe for light polarized with **E** parallel to **a** axis. Solid lines represent our data at room temperature and dashed lines represent the corresponding data reported in Ref. 25.

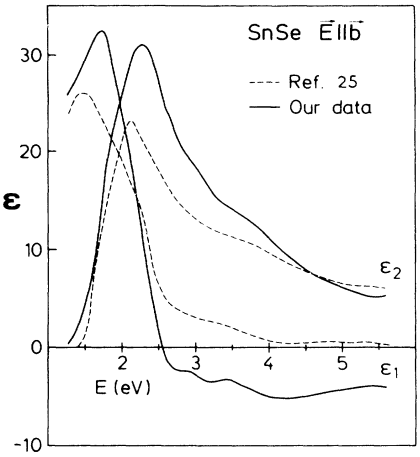

FIG. 3. Real and imaginary parts of the dielectric function ϵ_b. The symbols are the same as in Fig. 1.

TABLE I. Effective number of electrons per atom $n_{\text{eff}}(\omega_M)$ and static dielectric constant $\epsilon_{0,\text{eff}}(\omega_M)$ as given by sum rules and the parameters of oscillator energy E_0 and the interband strength E_d of Wemple and Di Domenico's model (Ref. 40).

	E‖a	E‖b
n_{eff}	1.48[a]	1.88[a]
	2.23[b]	2.27[b]
$\epsilon_{0,\text{eff}}$	9.96[a]	11.6[a]
	13.38[b]	14.9[b]
	13(2)[c]	17(2)[c]
E_0	2.52[b]	2.39[b]
E_d	31.16[b]	33.19[b]

[a]Reference 25; $\omega_M = 5.6$ eV.
[b]Our data; $\omega_M = 5.6$ eV.
[c]Reference 1; values obtained from the Kramers-Kronig analysis of infrared reflectivity.

difficult to prepare very thin samples. On the other hand, larger values in the imaginary part of the dielectric function in the ultraviolet region have been taken as a criterion for the quality of the spectroscopic ellipsometry measurements (i.e., for the IV and III-V semiconductors at E_2 energy region[26]). Our measurements satisfy this criterion. Additionally, in order to check the consistency of our spectra and compare them with the corresponding ones in Ref. 25 we have evaluated the sum rules for the oscillator strengths:

$$[\epsilon_{0,\text{eff}}(\omega_M)]_j = 1 + M^{-1}(\omega_M) ,$$

$$[n_{\text{eff}}(\omega_M)]_j = \frac{m}{4\pi e^2 N} M^1(\omega_M), \quad j=(a,b) ,$$

where

$$M^r(\omega_M) = \frac{2}{\pi} \int_0^{\omega_M} \omega^r \epsilon_2(\omega) d\omega ,$$

while $\epsilon_{0,\text{eff}}$ is the static dielectric constant and n_{eff} the number of electrons per atom contributing to the optical properties in the energy range $(0-\omega_M)$, and finally m and e are the mass and charge of the electron, respectively. The $\epsilon_{0,\text{eff}}$ values are expected to be very close to the experimental ϵ_0 values, because the convergence of the integral M^{-1} is very fast, if the sample is of a good quality without a surface oxide layer or other defects. The $\epsilon_{0,\text{eff}}$ values calculated from our data (see Table I), with $\omega_M = 5.6$ eV, for both polarizations **E‖a** and **E‖b** are very close to the experimental values of Ref. 1 obtained from the Kramers-Kronig analysis of infrared reflectivity. The corresponding values that we have found from the data of Ref. 25 are lower than our data and those of Ref. 1.

Our values of n_{eff} (=2.2/atom) at $\omega_M = 5.6$ eV are reasonably good compared with those for cubic SnTe (2/atom) (Ref. 27) at the same energy. We expect a slightly higher value for SnSe due to the substitution of the Te atoms by Se atoms with a higher electronegativity. One can notice from the data of Table I that the values of n_{eff} that we have calculated from the data of Ref. 25 are smaller even than those of SnTe. Thus we believe that our values for the $\epsilon_{0,\text{eff}}$ and n_{eff} are more reliable than those of Ref. 25, and because these values depend on the ϵ_2 and ϵ_1 spectra we conclude that our data are better than those of Ref. 25.

As in previous cases,[11,28] to perform a line-shape analysis of the structures in our SE spectra and thus to obtain the CP's parameters, we calculated numerically[29] the second-derivative spectra $(d^2\epsilon/d\omega^2)$. A least-squares procedure is utilized to fit simultaneously the real and imaginary parts of $d^2\epsilon/d\omega^2$ by using standard analytical expressions for the two-dimensional (2D) and three-dimensional (3D) CP line shapes:[30,31]

$$\epsilon \sim c - A \ln(E-\omega-i\Gamma)e^{i\Phi} \quad (2D) ,$$

$$\epsilon \sim c - A(\omega-E+i\Gamma)e^{i\Phi} \quad (3D) ,$$

where the excitonic angle Φ (Refs. 13 and 32) gives the amount of mixture of two critical points while E, Γ, and A represent the CP's energies, Lorenzian width and strengths, respectively.

Figure 4 shows the best fits of the second-derivatives of the real and imaginary parts together with the computed results from our experimentally obtained real part of the dielectric function for **E‖a** and **E‖b**. In Table II we have listed the CP's parameters and the type of the CP's, along with previous results from thermoreflectance and electroreflectance measurements.[2]

IV. CHANGES OF THE SURFACE OF GeS AND SnSe AFTER EXPOSURE TO AIR

Figure 5 shows the pseudodielectric function spectra measured by SE for the same SnSe sample for the polarization **E‖b** at an angle of incidence $\theta = 67.5°$. Each spectrum was obtained after the indicated time of exposure of the sample in the air. A 20-meV photon-energy mesh was used in all spectra and the time for each of them was about 11 min. The first spectrum was taken

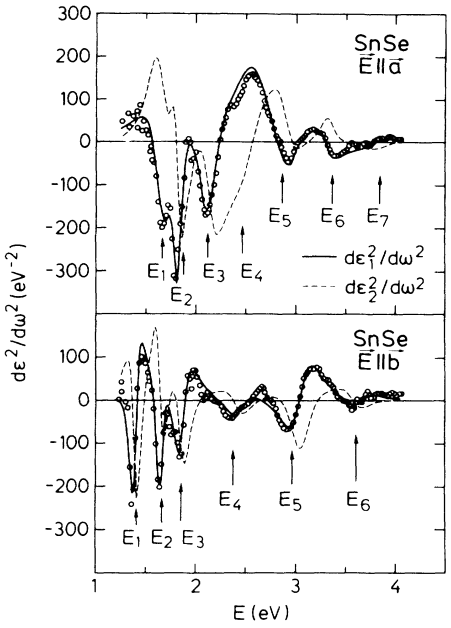

FIG. 4. Second derivatives of the real (solid line) and imaginary (dashed line) parts of the dielectric function of SnSe as a function of photon energy at room temperature, for the two studied polarizations. The experimental data are only given for $d^2\epsilon_1/d\omega^2$.

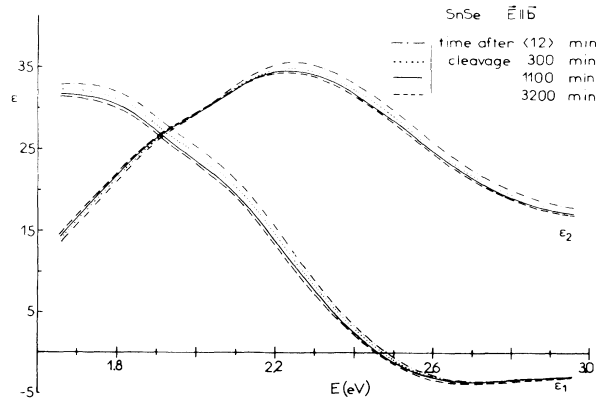

FIG. 5. The real and imaginary parts of the pseudodielectric function of SnSe from measurements with the bc plane of incidence perpendicular to the cleavage plane at an angle of incidence $\theta=67.5°$, and at different times after cleavage.

exactly 7 min after cleavage, the time that we need for the calibration of the instrument and to calculate the references of the polarizer and analyzer to the plane of incidence.[33] One can notice from this figure a large reduction in the real part of the pseudodielectric function ϵ_b in all the measured range, and a corresponding change in the imaginary part for energies larger than 2.1 eV, as the exposure time increases. The changes in the sample with time can be easily visualized through the changes in the ellipsometric angles Ψ and Δ (Ψ represents the relative changes of the amplitude upon oblique reflection, while Δ represents the relative changes in the phase).[23]

Figure 6 shows how the Ψ and Δ of SnSe change for both polarizations **E||a** and **E||b** versus exposure time. These measurements have been done with a null ellipsometer scheme at an angle of incidence $\theta=75°$ and at a wavelength $\lambda=6328$ Å on a freshly cleaved surface of

TABLE II. Critical-point energies, Lorentzian broadening parameters, and type of CP's in SnSe as well as results from cited references. Values are for room temperature.

Critical-point energy (eV)	Γ (meV)	Type of CP	Reference 2 thermore flectance	Reference 2 electrore flectance
		E||a polarization		
E_0			1.26	1.24
E_1 1.665(56)	170(56)	2D min. and saddle	1.66	1.65
1.758(17)	214(17)	2D min.		
E_2 1.813(35)	79(35)	2D min.	1.86	1.87
E_3 2.142(17)	145(17)	2D min. and saddle		
2.314(29)	304(29)	2D max. and saddle		
E_4 2.542(34)	333(34)	2D max. and saddle	2.44	
E_5 2.906(37)	206(37)	2D min. and saddle	3.06	
E_6 3.318(14)	111(14)	M_0 and M_3		
E_7 3.832(66)	341(66)	2D max. and saddle	3.88	
		E||b polarization		
E_0				1.05
E_1 1.353(21)	72(24)	2D min.		
E_2 1.641(29)	71(29)	2D min.		
E_3 1.861(41)	114(41)	2D min. and saddle	1.84	1.88
E_4 2.430(16)	134(30)	M_1	2.51	
E_5 3.056(18)	185(18)	2D max. and saddle	3.10	
E_6 3.584(49)	167(49)	2D min. and saddle	3.55	

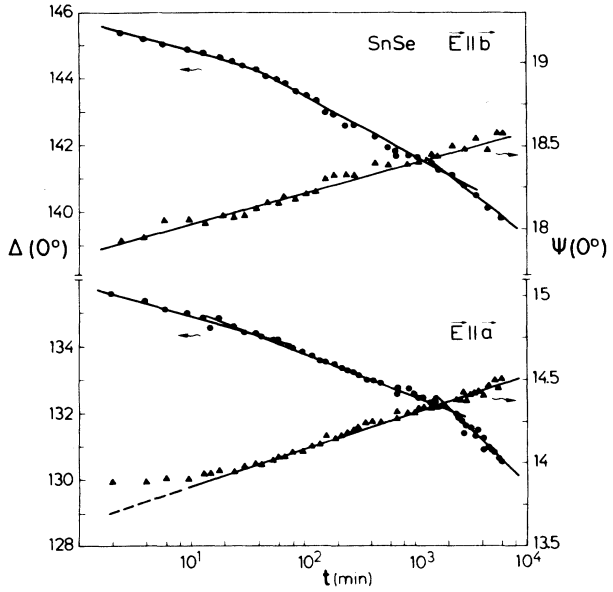

FIG. 6. The ellipsometric parameters Ψ and Δ of SnSe as a function of time at an angle of incidence $\theta=75°$ and $\lambda=6328$ Å. The time is measured from the moment of cleavage.

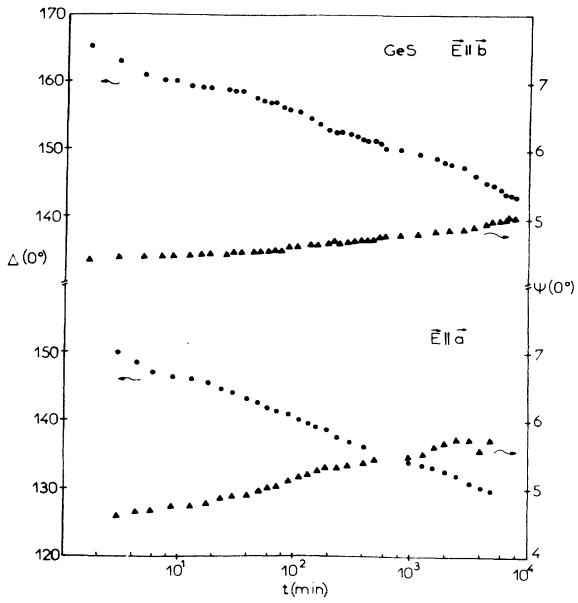

FIG. 7. The ellipsometric parameters Ψ and Δ of GeS as a function of the time. The symbols are the same as in Fig. 6.

SnSe and the time measured from the cleavage moment. These changes are surprisingly large and similar to those for polarization **E**∥**b** reported in Ref. 4 for GeS. We also show, in Fig. 7, the changes of the ellipsometric angles Ψ and Δ versus time for the case of the GeS for **E**∥**a** and **E**∥**b** axes. From the comparison of Figs. 6 and 7 we can see that the changes in the ellipsometric angles Ψ and Δ in the case of GeS are much larger than those of SnSe. For example, the changes of Δ in GeS are larger by a factor of 3 to 4 than those of SnSe.

These large changes for both materials exclude the formation of an overlayer produced by adsorption processes. Because the thickness of the adsorbed overlayer is usually some monolayers, the expected changes on the pseudodielectric function and the ellipsometric parameters Δ and Ψ would be very small.

In addition, RHEED was used to study the effect of exposure of the surface with time; the voltage used was 100 KeV. The RHEED patterns shown in Fig. 8 have been taken from the same area of a freshly cleaved sample of SnSe prepared for observations with this method, under the same orientation conditions, but at different times: (a) 7 min, (b) 43 min, and (c) 5100 min after cleavage. These patterns indicate that the diffraction spots become more diffuse and disappear with time [see Fig. 8(c)]. This effect implies that the formation of an amorphous layer on the freshly cleaved surface takes place. The thickness of this layer increases with time.

V. SIMPLE MODEL FOR THE ELECTRONIC STRUCTURE OF THE ⟨ 5*e* ⟩ ORTHORHOMBIC CRYSTALS

The electronic structure will be calculated using the LCAO method with nearest-neighbor interactions and an *s* and *p* orbital basis set. The Hamiltonian for the IV-VI orthorhombic compounds is a 32×32 matrix

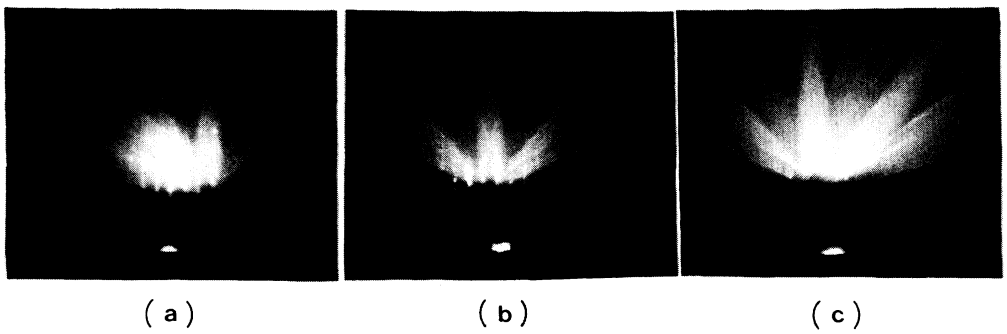

FIG. 8. Reflection electron diffraction photographs at different times: (a) 7 min, (b) 43 min, and (c) 5100 min after cleavage.

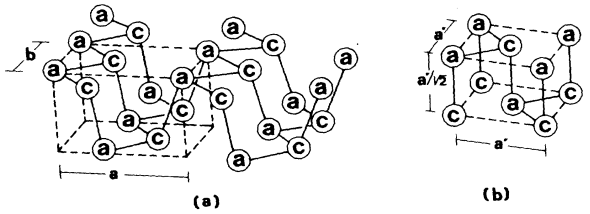

FIG. 9. (a) A double plane from the orthorhombic structure of the $\langle 5e \rangle$ crystals. a inside a circle denotes an anion atom, while c inside a circle denotes a cation atom. The two-dimensional (2D) unit cell of this double plane is outlined with dashed lines. (b) The simplified 2D unit cell for the double layer. All bond lengths are equal and all bond angles are set to 90°.

(16×16 for black-P) since there are eight atoms per unit cell (four for black-P). It is very difficult to obtain analytical solutions for the electronic structure. The orthorhombic structure can be considered as composed out of double planes. Each plane is composed out of zig-zag chains [Fig. 9(a)]. There are three bonds for each atom and one of them is shorter (by ~0.06 Å) than the other two (for black-P it is the other way around). Also the bond angles deviate from 90° (Table I in Ref. 22). One can assume that the main features of the electronic spectra arise from the fact that each atom is threefold coordinated. Therefore the following simplifications can be introduced. First we ignore the interlayer interactions, which correspond to third-neighbor interactions, and second, all bond lengths are considered to be equal and all bond angles are set to 90°. The resulting simple two-dimensional cell is depicted in Fig. 9(b). In this cell there are four atoms and each atom is fivefold coordinated. In the actual orthorhombic structure each atom is threefold coordinated. To incorporate this in the model, interactions are allowed only between atoms, which correspond to nearest-neighbor atoms in the original unit cell. The following orbitals are assumed to be centered on each atom: s, $p_+=(1/\sqrt{2})(p_x+p_y)$, $p_-=(1/\sqrt{2})(p_x-p_y)$, p_z. The interaction between the s and p orbitals (sp interaction) is very important in determining the electronic properties of the $\langle 5e \rangle$ crystals.[21,22] This interaction will be ignored at first, in order to find the essential features of the s and p bands. The different orbitals are now decoupled and only 4×4 Hamiltonian matrices have to be considered, one for each orbital. The eigenvalues can be computed in closed form. They are as follows.

s orbitals,

$$E=\frac{\varepsilon_s^c+\varepsilon_s^a}{2}\pm\left[\left(\frac{\varepsilon_s^c-\varepsilon_s^a}{2}\right)^2+V_{ss\sigma}^2[1+4\cos^2(\pi k_y)\pm4\cos(\pi k_x)\cos(\pi k_y)]\right]^{1/2}.$$

p_+ orbitals,

$$E=\frac{\varepsilon_p^c+\varepsilon_p^a}{2}\pm\left[\left(\frac{\varepsilon_p^c-\varepsilon_p^a}{2}\right)^2+V_{pp\sigma}^2+2V_{pp\pi}^2\{1\pm\cos[\pi(k_x+k_y)]\}+2V_{pp\sigma}V_{pp\pi}\{\cos(2\pi k_y)\pm\cos[\pi(k_x-k_y)]\}\right]^{1/2}$$

p_- orbitals,

$$E=\frac{\varepsilon_p^c+\varepsilon_p^a}{2}\pm\left[\left(\frac{\varepsilon_p^c-\varepsilon_p^a}{2}\right)^2+V_{pp\sigma}^2+2V_{pp\pi}^2\{1\pm\cos[\pi(k_x-k_y)]\}+2V_{pp\sigma}V_{pp\pi}\{\cos(2\pi k_y)\pm\cos[\pi(k_x+k_y)]\}\right]^{1/2}.$$

p_z orbitals,

$$E=\frac{\varepsilon_p^c+\varepsilon_p^a}{2}\pm\left[\left(\frac{\varepsilon_p^c-\varepsilon_p^a}{2}\right)^2+V_{pp\sigma}^2+4V_{pp\pi}^2\cos^2(\pi k_y)\pm4V_{pp\sigma}V_{pp\pi}\cos(\pi k_x)\cos(\pi k_y)\right]^{1/2}.$$

ε_s^c and ε_p^c are the term values for the s and p cation orbitals, respectively, while ε_s^a and ε_p^a are the similar term values for the anion. The relation $V_{pp\pi}=-V_{pp\sigma}/4$ is assumed to hold for the orthorhombic $\langle 5e \rangle$ crystals, as it was shown to hold for the cubic $\langle 5e \rangle$ crystals.[21] Consequently for black-P only three parameters are left to be evaluated, namely $\epsilon_p-\epsilon_s$, $V_{ss\sigma}$, and $V_{pp\sigma}$. These parameters will be determined by comparing the model bands to the black-P bands. To do this the s and p model bands are drawn separately in reduced units $(E-\epsilon_s)/V_{ss\sigma}$ and $(E-\epsilon_p)/V_{pp\sigma}$, respectively. One can make the following observations. The shape of the s bands closely resembles the s bands of black-P.[34–37] In fact, with only one parameter, i.e., $V_{ss\sigma}$ one can fit well the s bands of black-P. This result is plausible, since the s-electron bands are not sensitive to the details but to the topology of the structure. This is not the case for the p orbitals, because they are directional. As a consequence the p bands from the model are quite different from the black-P p bands.[34–37] However, upon close inspection, one can notice that they have some features in common. One such feature is a pair of bands, along the ΓX direction, which originates from the p_+ and p_- orbitals. This pair of bands is plotted with dashed lines in Fig. 10 third panel. In the actual orthorhombic structure, this pair of bands originates only from the p_y orbitals, since only these orbitals do not interact with the p_x and p_z ones when the wave vector has no component along the

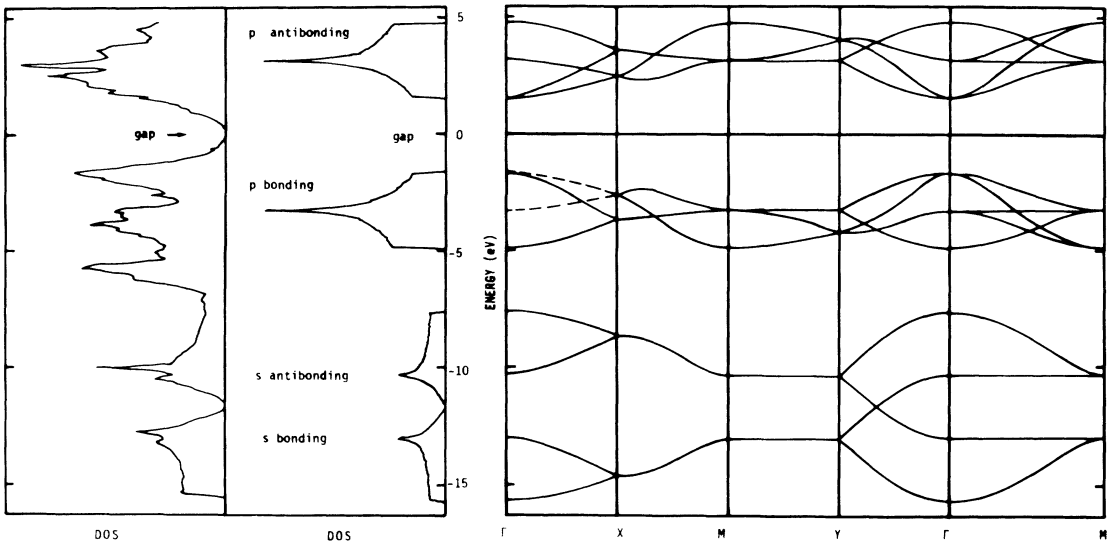

FIG. 10. Right and central panel: energy bands and density of states resulting from the simple model. Two-dimensional Brillouin zone as in Ref. 35. Left panel: density of states of black-P calculated using the LMTO method.

y axis. This pair of bands can be seen to appear in all the band-structure calculations for the orthorhombic $\langle 5e \rangle$ crystals.[14–17,36] For the case of black-P, this pair of bands has an energy separation, at Γ point of the Brillouin zone, equal to $V_{pp\sigma}/2$. Therefore, one can estimate $V_{pp\sigma}$ from the electronic structure of black-P,[37] which is calculated using the linear muffin-tin-orbitals method (LMTO).[38] The following value is obtained:

$$V_{pp\sigma}=3.2 \text{ eV} .$$

The $V_{ss\sigma}$ interaction can be estimated from the gap between the s bands at Γ point, which is equal to $2V_{ss\sigma}$. The following value is obtained from Ref. 37:

$$V_{ss\sigma}=1.34 \text{ eV} .$$

Also the energy separation between the s and p electron on-site matrix elements is estimated to be

$$\epsilon_p-\epsilon_s=-11.6 \text{ eV} .$$

In Fig. 10 the model bands (right panel), model (DOS) (central panel) and the DOS for black-P from Ref. 37 (left panel) are plotted. One can observe that the DOS shows four singularities (shown as sharp peaks) at energies $\epsilon_s \pm V_{ss\sigma}$ and $\epsilon_p \pm V_{pp\sigma}$. Three of them are in the valence bands and one in the conduction bands. In going to the actual black-P structure, these singularities will appear as sharp peaks. It can be noticed by comparison of the model DOS and the DOS of black-P (Ref. 37) that they both show two peaks in the DOS of the s band and that for the p valence bands our model shows one peak, while the DOS of black-P shows three. In going to the actual orthorhombic unit cell, all the bond lengths will no longer be equal and the bond angles will deviate from 90°. Then the orbitals p_+, p_-, and p_z will interact and the single peak will split into three main peaks.[37] If the sp interaction is also switched on, the uppermost peak will be pushed to higher energies, as in the case of the $\langle 5e \rangle$ cubic compounds.[21] The bandwidth of the valence bands will also increase and the gap between the valence bands and the conduction bands will decrease. The above changes are going to affect the polarizability of the crystals and the energy where the maximum of the imaginary part of the dielectric constant occurs.

It is reasonable to assume that the bonding in the simple model is produced through σ bonds between orbitals of the same type, i.e., p_+, p_+, centered on nearest-neighbor atoms. The bond energy is equal to

$$\epsilon_{b0}=-\left[\left[\frac{\varepsilon_p^c-\varepsilon_p^a}{2}\right]^2+V_{pp\sigma}^2\right] .$$

Such a bond picture is compatible with the model electronic band structure[37] (Fig. 10). The bonds interact between themselves through the $V_{pp\pi}$ interaction. This interaction is responsible for the formation of the bands. We can estimate the bond energy for all the $\langle 5e \rangle$ orthorhombic compounds by taking ε_p^c and ε_p^a to be the appropriate term values[39] and $V_{pp\sigma}$ to be given by the following relation:[40]

$$V_{pp\sigma}=V_{pp\sigma}^0(d_0/d)^2 ,$$

where d is the nearest-neighbor distance, and $V_{pp\sigma}^0$ and d_0 refer to the corresponding values for black-P. To compare these estimates with the experiment, let us suppose that a single oscillator dominates the optical transitions with an energy $E_g=2\epsilon_{b0}$. As a result, the dielectric constant ϵ_0 given by the relation[41]

$$\epsilon_0=1+\frac{\hbar^2 4\pi Ne^2}{mVE_g^2} ,$$

TABLE III. Calculated bond energies, average gaps, and dielectric constants for the orthorhombic $\langle 5e \rangle$ compounds.

	$V_{pp\sigma}$	$(\varepsilon_p^c - \varepsilon_p^a)/2$	ϵ_{b0}	E_g (eV)	ϵ_0	E‖a	E‖b	E‖c
P	3.20	0	3.20	6.40	9.23[a]	16.5[b]	13.0[b]	8.3[b]
GeS	2.59	1.96	3.25	6.50	9.00[a]	14.8[c]	12.0[c]	10.0[c]
						9.49[d]	10.01[d]	7.91[d]
GeSe	2.42	1.59	2.90	5.79	9.98[a]	18.7[e]	21.9[e]	14.4[e]
SnS	2.30	2.17	3.16	6.32	8.12[a]	14[f]	16[f]	16[f]
SnSe	2.07	1.80	2.75	5.49	9.47[a]	13[f]	17[f]	16[f]
						13.4[g]	14.9[g]	

[a]Calculated values.
[b]Reference 42.
[c]Reference 1.
[d]Reference 12.
[e]Reference 43.
[f]Reference 1.
[g]Our data.

where V is the volume of the unit cell and $N=40$, is the number of the electrons in each unit cell. All the bonds in the model are equivalent and it can be shown that this leads to isotropic dielectric properties. This is in agreement with the experiments[25] which do not indicate any anisotropy in the ϵ_2 spectrum above 3 eV. In Table III the calculated E_g and ϵ_0 are given together with all the necessary data and the experimental dielectric constant tensor. The calculated values for ϵ_0 are close to the experimental ones, and the trend in the values is correctly given. The compound with the highest ϵ_0 is GeSe. Also, the experimental results given in Table III do not show large anisotropy in ϵ_0 except for the case of black-P. This anisotropy is due to transitions from the upper valence states to the conduction states and depend upon the details of the crystal structure.

The energy E_g has the same meaning as the bonding-antibonding gap in the crystals with an average of four electrons per atom ($\langle 4e \rangle$)[44], i.e., III-V compounds. The difference is that in the present case it corresponds to σ bonded p orbitals, while for the $\langle 4e \rangle$ crystals to σ bonded sp^3 hybrids. It is interesting to see whether the present energy gap E_g has any correlation with energy position of the maximum of ϵ_2. For the crystals with $\langle 4e \rangle$ it has been found the maximum of ϵ_2 occurs at energies close to E_g. From the known spectra and the present results, the maximum of ϵ_2 is at energies half the E_g value, while at energies close to E_g the ϵ_2 changes slope, which indicates the presence of additional transitions. As we have noted before in going to the actual orthorhombic structure and switching on the sp interaction, the main p bonding peak in the model DOS splits into three main peaks. The dielectric properties would then be dominated by transitions from the peak lying at the top of the valence bands to the conduction bands, and the maximum of ϵ_2 is going to appear at energies lower than the calculated E_g. Also, the above can be used to explain why the calculated ϵ_0 is systematically lower than the experimental results.

VI. CONCLUSIONS

The room-temperature dielectric function of orthorhombic SnSe, for the electric field vector **E** parallel to the **a** and **b** axes, is measured and analyzed. The critical-point parameters are found to show similar features with those of GeS. Exposure to air of GeS and SnSe is found to have a profound effect on the pseudodielectric constant and the ellipsometric parameters. From our data it can be inferred that an amorphous overlayer is formed. This overlayer grows much more rapidly on GeS than on SnSe. Additional measurements are needed to determine the chemical nature of the overlayer. For the case of GeS it is possible that the overlayer is amorphous Ge_xS_{1-x} which is 4:2 coordinated and satisfies the coordination of Ge and S better than crystalline GeS.

A simple model for the electronic structure and the bonds of the orthorhombic $\langle 5e \rangle$ crystals is proposed. The model is based on the LCAO method. Analytical expressions are given for the electronic energies. The interatomic interactions are determined using these analytical expressions and the known band-structure calculations for black-P. The bond energy is determined for all the orthorhombic $\langle 5e \rangle$ crystals. Thus estimates for the dielectric constant were calculated. The resulting values are in semiquantitative agreement with the experimental results.

ACKNOWLEDGMENTS

One of us (S.L.) is indebted to Professor M. Cardona for his hospitality in the Max-Planck-Institut für Festkörperforschung, Stuttgart, Germany, where some of the measurements were performed. Also, we would like to thank Professor J. Stoemenos for the RHEED observations and stimulating discussions, as well as E. Schönherr for the growth of the crystals and E. Kisela and his group at the Max-Planck-Institut for the sample preparation. We also thank Dr. N. K. Flevaris for his critical reading of this manuscript.

[1]J. D. Wiley, W. J. Buckel, and R. L. Schmidt, Phys. Rev. B **13**, 2489 (1976); H. R. Chandrasekhar, R. G. Humphreys, U. Zwick, and M. Cardona, *ibid.* **15**, 2177 (1977).
[2]F. Lukes, J. Humlicek, and E. Schmidt, Solid State Commun. **45**, 445 (1983); G. Valiukonis, F. M. Gashimzade, D. A. Guseinova, G. Krivaite, A. M. Kulibekov, G. S. Orudcev, and A. Sileika, Phys. Status Solidi B **117**, 81 (1983); G. Valiukonis, F. M. Gashimzade, D. A. Guseinova, G. Krivaite, M. M. Mamedov, and A. Sileika, Phys. Status Solidi B **122**, 623 (1984).
[3]I. Gregora, B. Velicky, and M. Zavetova, J. Phys. Chem. Solids **37**, 785 (1976).
[4]F. Lukes, E. Schmidt, J. Humlicek, and P. Dub, Phys. Status Solidi B **122**, 675 (1984).
[5]J. D. Wiley, D. Thomas, E. Schonher, and A. Breitscwerdt, J. Phys. Chem. Solids **41**, 801 (1979).
[6]D. E. Aspnes, in *Optical Properties of Solids,* edited by Abeles (North-Holland, Amsterdam, 1969), Chap. 15.
[7]D. E. Aspnes and A. A. Studna, Phys. Rev. B **27**, 985 (1983), and references therein.
[8]W. E. J. Neal, Appl. Surf. Sci. **2**, 445 (1979).
[9]D. E. Aspnes, J. Opt. Soc. Am. **70**, 1275 (1980).
[10]G. Jungk and A. Roseler, Phys. Status Solidi B **123**, 65 (1984).
[11]L. Vina, S. Logothetidis, and M. Cardona, Phys. Rev. B **30**, 1979 (1984); S. Logothetidis, Ph.D. thesis, University of Thessaloniki, Greece, 1984 (unpublished).
[12]S. Logothetidis, L. Vina, and M. Cardona, Phys. Rev. B **31**, 2180 (1985).
[13]S. Logothetidis, P. Lautenschlager, and M. Cardona, Phys. Rev. B **33**, 1110 (1986).
[14]L. Abbati, L. Baicovich, G. Ciucci, R. Car, and L. Quartapelle, Nuovo Cimento **39**, 727 (1977).
[15]T. Grandke and L. Ley, Phys. Rev. B **16**, 832 (1977).
[16]R. Car, G. Ciucci, and L. Quartapelle, Phys. Status Solidi B **86**, 471 (1978).
[17]G. Ciucci, A. Guarnieri, G. L. Masserini, and L. Quartapelle, Solid State Commun. **29**, 75 (1979).
[18]A. Bussmann-Holder, H. Bilz, and P. Vogl, in *Dynamical Properties of IV-VI, Compounds,* Vol. 99 of *Springer Tracts in Modern Physics* (Springer, Berlin, 1983).
[19]D. R. Lovett, *Semimetals and Narrow-Bandgap Semiconductors* (Pion Limited, London, 1977).
[20]A. Morita, Appl. Phys. A **39**, 227 (1986).
[21]H. M. Polatoglou, G. Theodorou, and N. A. Economou, Phys. Rev. B **33**, 1265 (1986).
[22]H. M. Polatoglou, Phys. Rev. B **33**, 5865 (1986).
[23]R. M. A. Azzam and N. M. Bashara, *Ellipsometry and polarized Light* (North-Holland, Amsterdam, 1977).
[24]D. E. Aspnes, J. C. Phillips, K. L. Tai, and P. M. Bridenbaugh, Phys. Rev. B **23**, 816 (1981).
[25]R. Eymard and A. Otto, Phys. Rev. B **16**, 1616 (1977).
[26]D. E. Aspnes and A. A. Studna, Phys. Rev. B **27**, 985 (1983).
[27]M. Cardona, J. Appl. Phys. **36**, 2181 (1965).
[28]S. Logothetidis, L. Vina, and M. Cardona, Phys. Rev. B **31**, 947 (1985); L. Vina, H. Hochst, and M. Cardona, *ibid.* **31**, 958 (1985).
[29]A. Savitzky and J. C. Golay, Anal. Chem. **36**, 1627 (1964); J. Steinier, Y. Termonia, and J. Deltour, *ibid.* **44**, 1906 (1972).
[30]M. Cardona, *Modulation Spectroscopy* (Academic, New York, 1969), Suppl. 11.
[31]J. E. Rowe and D. E. Aspnes, Phys. Rev. Lett. **25**, 162 (1970).
[32]Y. Toyozawa, M. Inoue, T. Inui, M. Okazaki, and E. Hanamura, J. Phys. Soc. Jpn. **22**, 1337 (1967).
[33]L. Vina, Ph. D. thesis, University of Stuttgart, 1985.
[34]H. Asahiro and A. Morita, J. Phys. Soc. Jpn. **49**, Suppl A, 85 (1980).
[35]Y. Takao and A. Morita, Physica **105B**, 93 (1981).
[36]H. Asahina and A. Morita, J. Phys. C **17**, 1839 (1984).
[37]H. M. Polatoglou, and M. Methfessel (unpublished).
[38]O. K. Andersen, Phys. Rev. **12**, 3060 (1975).
[39]F. Herman, and S. Skillman, *Atomic Structure Calculations* (Prentice-Hall, Englewood Cliffs, NJ, 1963).
[40]W. A. Harrison, *Electronic Structure and the Properties of Solids* (Freeman, San Francisco, 1980).
[41]M. Cardona, in *Atomic Structure and Properties of Solids,* edited by E. Burstein (Academic, New York, 1972), p. 514.
[42]T. Nagahama, M. Kobayashi, Y. Akahama, S. Endo, and S. Narita, J. Phys. Soc. Jpn. **54**, 2096 (1985).
[43]H. R. Chandrasekhar and U. Zwick, Solid State Commun. **18**, 1509 (1976).
[44]J. C. Phillips, *Bonds and Bands in Semiconductors* (Academic, New York, 1973).

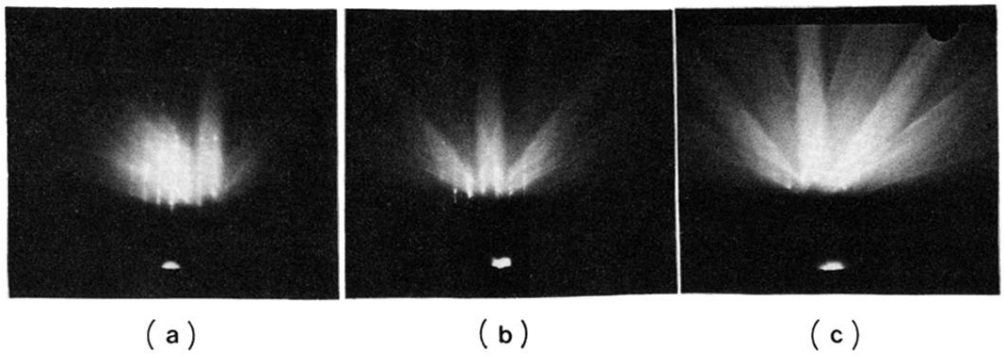

FIG. 8. Reflection electron diffraction photographs at different times: (a) 7 min, (b) 43 min, and (c) 5100 min after cleavage.